

Altered Structural Connectome in Temporal Lobe Epilepsy¹

Matthew N. DeSalvo, MD
Linda Douw, PhD
Naoaki Tanaka, MD, PhD
Claus Reinsberger, MD, PhD
Steven M. Stuffelbeam, MD

Purpose:

To study differences in the whole-brain structural connectomes of patients with left temporal lobe epilepsy (TLE) and healthy control subjects.

Materials and Methods:

This study was approved by the institutional review board, and all individuals gave signed informed consent. Sixty-direction diffusion-tensor imaging and magnetization-prepared rapid acquisition gradient-echo (MP-RAGE) magnetic resonance imaging volumes were analyzed in 24 patients with left TLE and in 24 healthy control subjects. MP-RAGE volumes were segmented into 1015 regions of interest (ROIs) spanning the entire brain. Deterministic white matter tractography was performed after voxelwise tensor calculation. Weighted structural connectivity matrices were generated by using the pairwise density of connecting fibers between ROIs. Graph theoretical measures of connectivity networks were compared between groups by using linear models with permutation testing.

Results:

Patients with TLE had 22%–45% reduced ($P < .01$) distant connectivity in the medial orbitofrontal cortex, temporal cortex, posterior cingulate cortex, and precuneus, compared with that in healthy subjects. However, local connectivity, as measured by means of network efficiency, was increased by 85%–270% ($P < .01$) in the medial and lateral frontal cortices, insular cortex, posterior cingulate cortex, precuneus, and occipital cortex in patients with TLE as compared with healthy subjects.

Conclusion:

This study suggests that TLE involves altered structural connectivity in a network that reaches beyond the temporal lobe, especially in the default mode network.

© RSNA, 2013

Online supplemental material is available for this article.

¹From the Athinoula A. Martinos Center for Biomedical Imaging, 149 Thirteenth St, Suite 2301, Charlestown, MA 02129 (M.N.D., L.D., N.T., C.R., S.M.S.); Department of Radiology, Massachusetts General Hospital, Charlestown, Mass (M.N.D., L.D., N.T., S.M.S.); and Department of Neurology, Brigham and Women's Hospital, Boston, Mass (C.R.). Received May 6, 2013; revision requested June 9; revision received July 9; accepted July 19; final version accepted August 22. Supported by the National Center for Research Resources, the National Institutes of Health Human Connectome Project, the Mental Illness and Neuroscience Discovery Institute, the Netherlands Organisation for Scientific Research (NOW) Rubicon grant, the Epilepsy Foundation of America, the Japan Epilepsy Research Foundation, and an RSNA Research Medical Student Grant. Address correspondence to S.M.S. (e-mail: sms@nmr.mgh.harvard.edu).

Temporal lobe epilepsy (TLE) is the most common type of epilepsy and accounts for about half of all cases of focal epilepsy. Although classically, TLE has been theorized to relate to isolated injury of temporal structures, such as the hippocampus and amygdala, more recent studies have demonstrated widespread cortical atrophy, involving both temporal and extratemporal areas, leading to the concept of TLE as a “network disease” (1). The default mode network (DMN), which was first characterized by Raichle et al (2) as the set of brain regions activated during task-free introspection and deactivated during goal-directed behavior, has been consistently found to be among the extratemporal areas affected by TLE in studies of structural and functional connectivity, which may explain certain cognitive and psychiatric symptoms in patients with TLE (3–5). High-resolution structural magnetic resonance (MR) imaging has also shown cortical thinning in the DMN in patients with TLE, which suggests an altered pattern of long-range connectivity (6,7).

Diffusion-tensor imaging has been used to study white matter microstructure in TLE in multiple prior studies. These studies have been largely focused on measures of fractional anisotropy to characterize tract integrity. Decreased anisotropy has been observed in widespread tracts, including bilateral uncinate, arcuate, inferior fronto-occipital,

and superior longitudinal and inferior longitudinal fasciculi, as well as the corticospinal tract, fornix, cingulum, and anterior thalamic radiation (8,9). Although these studies have led to new insights into the pathophysiology of TLE, it has become apparent that a complementary network approach is necessary to study the complex interplay of changes in structural connectivity throughout the brain in TLE.

Connectomics is a new field, focused on quantifying and formally analyzing properties of complex large-scale connectivity networks created by using structural and functional neuroimaging techniques (10). In this approach, brain regions are represented as nodes of a graph with connecting edges, based on measures of either functional or structural connectivity. Graph theory is used to quantify and compare properties of these networks. For example, although the brain has been described as modular for many decades, only within recent years has the structural modularity of brain networks been quantitatively described with graph theory (11). Another key discovery of these efforts was that cortical areas of the DMN act as the structural hubs of the human brain (11). Although structural networks have not been studied extensively in the setting of pathology, altered structural connectivity in brain networks may represent a biomarker for a variety of neuropsychiatric conditions (12,13).

Thus, although TLE has been traditionally theorized to relate to isolated injury of temporal structures, recent studies have demonstrated widespread cortical atrophy and loss of white matter integrity involving both temporal and extratemporal areas, especially among areas of the DMN, leading to the concept of TLE as a network disease. We

investigated differences in the whole-brain structural connectomes in patients with TLE and healthy control subjects.

Materials and Methods

Subjects

Data were reviewed retrospectively and analyzed for 24 patients with left TLE (duration of epilepsy ranging from 1 to 52 years; mean, 17 years) and 24 healthy control subjects who were matched for age, sex, and handedness and were evaluated between April 2007 and December 2012. Patients were included if they received a clinical diagnosis of left TLE and were referred for advanced neuroimaging (including diffusion-tensor imaging) as part of presurgical evaluation by means of a multidisciplinary consensus conference. In addition to clinical and MR imaging evaluations, patients received diagnoses on the basis of long-term video and electroencephalographic, or EEG, monitoring (24 of 24 patients), positron emission tomography (20 of 24 patients), magnetoencephalography (14 of 24 patients), intracranial EEG (14 of 24 patients), and single-photon emission



Advances in Knowledge

- In patients with left temporal lobe epilepsy (TLE) compared with control subjects, we observed 22%–45% decreases ($P < .01$) in long-range connectivity among areas of the default mode network (DMN), which has been previously identified as the structural hub of the human brain.
- We observed widespread 85%–270% increases ($P < .01$) in local connectivity within and beyond the DMN, which we hypothesize is caused by loss in white matter integrity and chaotic fiber directionality.

Implication for Patient Care

- TLE involves alterations in structure beyond the medial temporal lobe, especially in the DMN, that may provide a noninvasive biomarker for diagnosis, prognosis, and therapy monitoring in patients with TLE.

Published online before print

10.1148/radiol.13131044 **Content codes:**  

Radiology 2014; 270:842–848

Abbreviations:

DMN = default mode network
MP-RAGE = magnetization-prepared rapid acquisition gradient-echo
ROI = region of interest
TLE = temporal lobe epilepsy

Author contributions:

Guarantors of integrity of entire study, M.N.D., N.T., S.M.S.; study concepts/study design or data acquisition or data analysis/interpretation, all authors; manuscript drafting or manuscript revision for important intellectual content, all authors; approval of final version of submitted manuscript, all authors; literature research, all authors; clinical studies, M.N.D., N.T., C.R.; experimental studies, N.T., C.R., S.M.S.; statistical analysis, all authors; and manuscript editing, all authors

Funding:

This research was supported by the National Institutes of Health (grants P41-RR14075, R01-NS037462, R01-NS069696, and 5R01-NS060918).

Conflicts of interest are listed at the end of this article.

computed tomography (three of 24 patients). Among those that later underwent left anterior temporal lobectomy, pathologic substrates were determined to be mesial temporal sclerosis in eight patients and gliosis in three. Two patients had structural brain lesions (with the exception of mesial temporal sclerosis in 12 patients), and four patients had undergone prior neurosurgery and were excluded from the study. Healthy control subjects were recruited from the community. This study was approved by our institutional review board, and all individuals gave signed informed consent.

All study subjects were assessed clinically by an epileptologist (N.T., with 11 years of experience), who was unaware of imaging results at the time of assessment.

MR Imaging Acquisition

MR imaging was performed with a 3-T Tim Trio system (Siemens, Erlangen, Germany) with a vendor-produced 32-channel head coil. High-resolution T1-weighted magnetization-prepared rapid acquisition gradient-echo (MP-RAGE) sequences were performed with a repetition time (msec)/echo time (msec) of 2530/1.74 and a flip angle of 70°, resulting in a matrix of 256 × 256 × 176 isotropic 1-mm voxels. Single-shot echo-planar diffusion-weighted images were acquired with 8080/83 and flip angle of 90°, resulting in matrices of 128 × 128 × 64 isotropic 1.85-mm voxels. Ten b_0 volumes and 60 directional gradients at $b = 700 \text{ sec/mm}^2$ were acquired.

All MR images were evaluated by a neuroradiologist (S.M.S., with 15 years of experience).

Segmentation, Parcellation, and Tractography

The details of the methods used are described in Hagmann et al (11) and Dadduci et al (14) and will be described briefly here. The MP-RAGE volumes were registered to the b_0 volumes by using a rigid body alignment with the FLIRT tool (the FMRIB [Functional Magnetic Resonance Imaging of the Brain] Linear Image Registration Tool) from the FSL (FMRIB Software Library) Toolbox (University of Oxford, Oxford, England). FreeSurfer

version 5 software (<http://surfer.nmr.mgh.harvard.edu>) was used to parcellate the cortical surface representations, segment gray and white matter (15,16), and define 34 cortical regions of interest (ROIs) per hemisphere and 15 subcortical ROIs by using T1-weighted images with the Desikan-Killiany atlas (17). Cortical surfaces were further divided into 1000 ROIs with about a 1.5-cm² surface area that spanned the entire cortex (Fig 1) by using Connectome Mapper Lausanne 2008 parcellation (www.connectomics.org) for a total of 1015 cortical and subcortical ROIs. The diffusion data were inspected visually for motion, and only data without visible motion were included for analysis. Tensor data were reconstructed by using the Diffusion Toolkit (www.trackvis.org/dtk). A classic deterministic streamline fiber-tracking algorithm provided by the Connectome Mapper (18) (angle threshold = 60°) was performed on the entire white matter by using 32 random seed points per voxel (14). Fibers shorter than 2 cm and longer than 50 cm were removed, and all remaining fibers were spline-filtered for smoothing.

Network Construction

A weighted structural connectivity adjacency matrix was created for each subject (Fig 1) by considering each ROI as a node connected by edges weighted by the density of connecting fibers, calculated as follows:

$$w(e) = \frac{2}{S_u + S_v} \sum_{f_c} \frac{1}{l(f_c)}$$

where nodes u and v have white matter surface areas S_u and S_v , respectively, and are connected by fibers f_c with lengths $l(f_c)$. The use of the factor $l(f_c)$ to correct for linear bias toward longer fibers introduced by tractography has been validated to lead to reduced intrasubject variability between imaging examinations (19).

Network Analysis with Graph Theory

Global and nodal network properties were calculated by using the Brain Connectivity Toolbox (<https://sites.google.com/site/bctnet/>):

Degree: Degree is a nodal property defined as the number of connections, or nonzero edges, that involve that node.

Efficiency: Global efficiency is the average across all nodes of the inverse shortest path length (d_{uv})—networks with short path lengths are more efficient. Local efficiency (E_u) is computed for a node u as the average inverse path length (d_{uv}) between u and nodes v .

Modularity: We applied the Newman spectral algorithm (20) to detect modules by maximizing within-community connectivity while minimizing between-group connectivity by using the following formulas:

$$E_u = \frac{1}{N-1} \sum_{u \neq v} \frac{1}{d_{uv}} \quad \text{and}$$

$$Q = \frac{1}{4m} \sum_{uv} \left(A_{uv} - \frac{k_u k_v}{2m} \right) s_u s_v,$$

where Q is overall network modularity, A_{uv} is the number of edges between nodes u and v , m is the total number of edges in the network, k_u is the degree of u , and S_u and S_v are group membership variables for nodes u and v . Within-module connectivity was assessed by calculating within-module z score of degree for each node, while between-module connectivity was measured by using the participation coefficient:

$$P_u = 1 - \sum_M \left(\frac{\kappa_{us}}{k_u} \right)^2,$$

where M is the set of all modules identified and κ_{us} is the number of edges from u to nodes within module s . To better understand the anatomic distribution of these modules, we applied the same algorithm to an adjacency matrix computed by taking the mean connectivity value for each ROI pair across all individuals (both healthy subjects and patients with TLE) and displayed these modules as color-coded regions on a cortical surface template by using FreeSurfer software (Fig 2).

Statistics

Graph measures were statistically compared across groups by using a linear

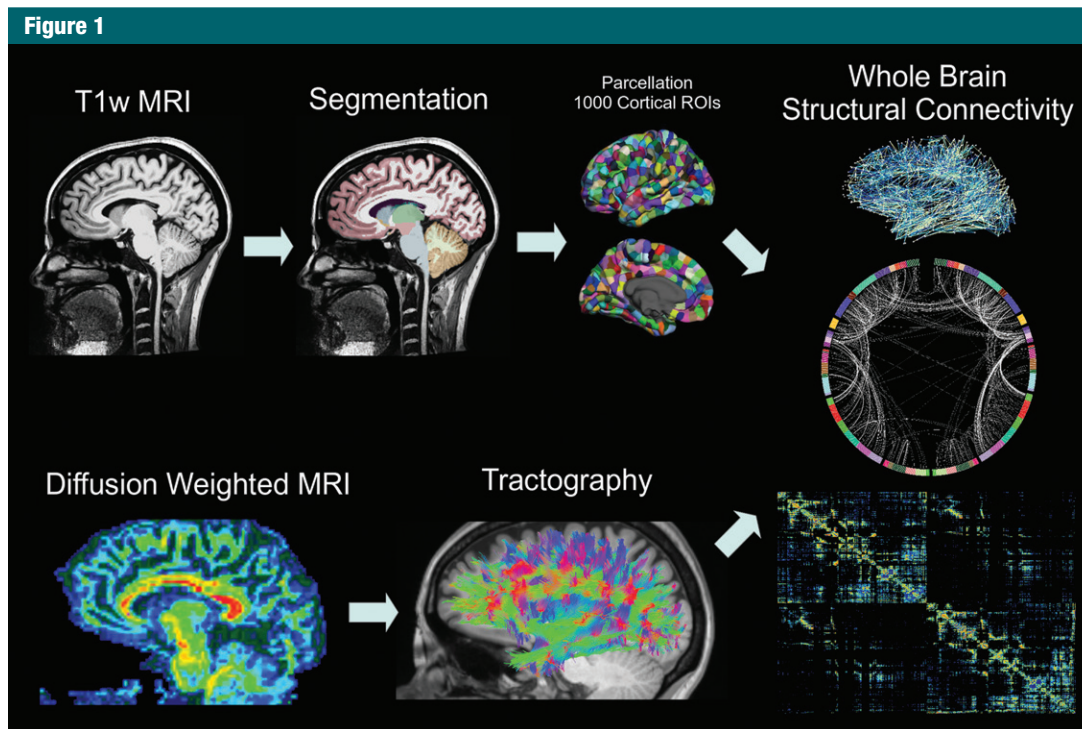


Figure 1: Flowchart illustrates the steps of the connectivity analysis. MP-RAGE volumes are segmented into 83 ROIs, which are further parcellated into 1000 cortical and 15 subcortical ROIs. Whole-brain white matter tractography is performed after voxelwise tensor calculation, and the density of fibers that connect each pair of cortical ROIs is used to calculate structural connectivity. *T1w* = T1-weighted.

model, with age and sex included as nuisance variables. In each model, the graph measure was the response variable, while the fixed effects of age, sex, and group (TLE or control group) were measured as predictors. The hypothesis that each graph measure satisfied a Gaussian distribution was tested by using a one-sample Kolmogorov-Smirnov test. To correct for multiple comparisons, an empirical estimate of the null distribution was calculated for each network property studied by randomly permuting individuals between groups and recording the number of supra-threshold ($P < .05$) ROIs across 10000 iterations. We then used these empirical null distributions to calculate a corrected P value for the effect of group (TLE or control group) at each ROI and thresholded the final results at $P < .01$. In separate analyses, the effects of presence of mesial temporal sclerosis (as a binary variable), as well as duration of epilepsy, were each added to the

linear model as predictors. The hypothesis that the mean age was different between groups was tested by using a two-sample t test. We tested the normality of each age distribution with a one-sample Kolmogorov-Smirnov test. We tested the hypothesis that sex and handedness were different between groups by using the Fisher exact test. All statistical analyses were performed with MATLAB R2012b (Mathworks, Natick, Mass).

Results

Participant Characteristics

Statistical comparison of groupwise differences in participant characteristics between the TLE group (age range, 12–65 years [mean age \pm standard deviation, 33 years \pm 16.5]; 10 men [age range, 12–59 years; mean age, 32 years] and 14 women [age range, 14–65 years; mean age, 33 years], 21 of

whom were right handed) and healthy subject group (age range, 19–55 years [mean age, 25 years \pm 9]; nine men [age range, 19–50 years; mean age, 24 years] and 15 women [age range, 20–55 years; mean age, 26 years], 24 of whom were right handed) demonstrated that there was no significant difference in mean age ($t = 1.90$, $P > .05$), sex ($P > .99$), or handedness ($P > .23$) distribution between patients with TLE and healthy subjects in this study.

Modularity

Overall network modularity was not significant ($P > .05$) between groups. Modularity analysis of the across-subjects mean adjacency matrix yielded seven large, approximately symmetrical modules: (a) left frontal, (b) right frontal, (c) left parietal, (d) right parietal, (e) left temporo-occipital, and (f) right temporo-occipital modules, as well as (g) a single medial frontoparietal module that included the bilateral superior

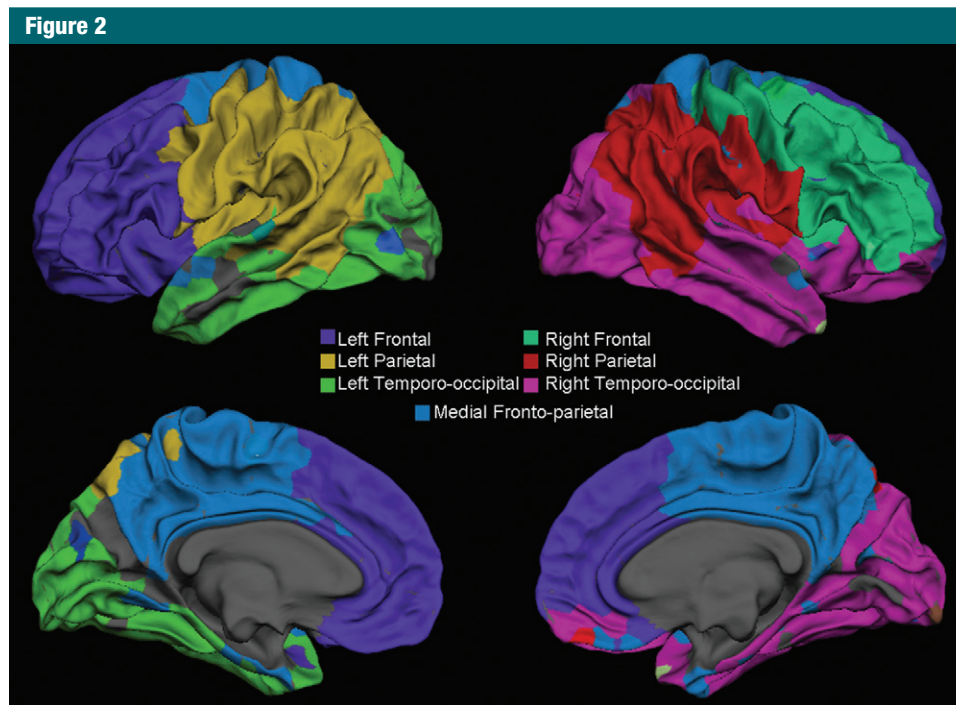


Figure 2: Surface representation shows the gray–white matter junction of the seven modules that emerge by using the Newman spectral algorithm on an across-subject (both healthy subjects and patients with TLE) average connectivity matrix.

frontal gyri, posterior cingulate cortices, and precunei, with a few connections to bilateral medial and lateral temporal areas (Fig 2).

Structural Connectivity

Both within- and between-module connectivity were decreased ($P < .01$) in the medial orbitofrontal cortex, precuneus, and posterior cingulate cortex in the setting of TLE (Fig 3). Decreased ($P < .01$) between-module connectivity was also observed in bilateral lateral frontal, inferior parietal, medial orbitofrontal, and temporal cortices in patients with TLE. Global network efficiency was increased in the setting of TLE ($P < .001$). Local efficiency was increased ($P < .01$) in bilateral precuneus and posterior cingulate cortices, as well as in lateral frontal, temporal, insular, and occipital cortices in the setting of TLE (Fig 3). The ROIs with significant changes in network properties are shown in Tables E1–E3 (online). Neither presence of mesial temporal sclerosis nor duration of epilepsy was

associated ($P > .05$) with differences in graph properties among patients with TLE.

Discussion

With diffusion MR imaging, we found alterations in the structural connectivity of distributed cortical regions in patients with TLE. Our principal finding was that structural connectivity was decreased throughout the DMN, as measured with both within-module and between-module connectivity. This suggests that the DMN may have a reduced role as the structural hub of brain connectivity in patients with TLE. This result is supported by prior functional MR imaging studies that have shown decreased functional connectivity in DMN areas in TLE (4,5).

Our finding of disrupted hub connectivity among DMN areas is also supported by a prior study in which diffusion-tensor imaging was used to show decreased fractional anisotropy along the cingulum tract (3). This

altered pattern of long-range connectivity may underlie the pathophysiology of epileptiform activity propagation that may reinforce an altered TLE network. Changes in structural connectivity may also be related to distant effects, such as cortical thinning in the DMN (6,7).

In addition to decreased structural connectivity in DMN areas, we also observed widespread increases in local and global connectivity (efficiency) in and beyond the DMN in the cerebral cortices of patients with TLE. This suggests that the pathways of neural activity are more efficient (or connected) than those in healthy populations, which may allow epileptiform discharges to propagate. Given the finding of decreased long-range DMN connectivity, this increased local connectivity may appear paradoxical initially.

These current findings, however, might be reconciled by considering the relative scales of each connectivity measure used in this study. Local efficiency, which primarily measures the connectivity in the immediate vicinity of

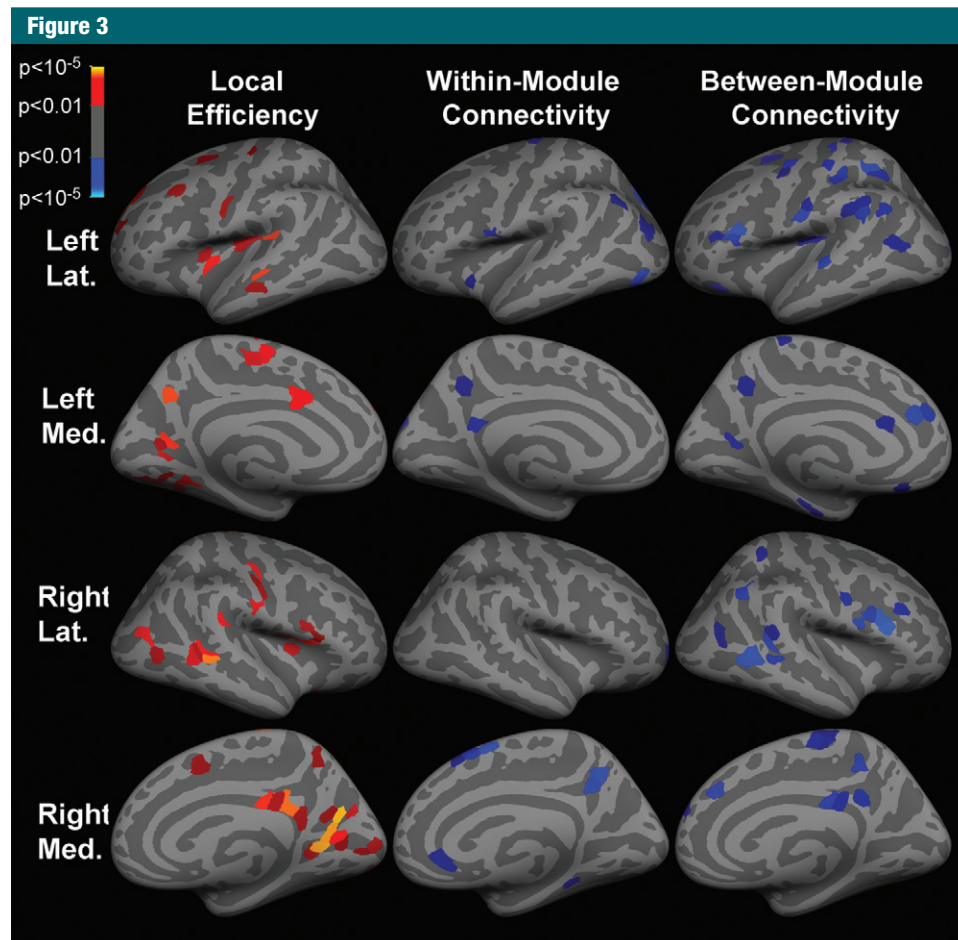


Figure 3: Inflated cortical surface representations show the significant ($P < .01$) differences in graph theoretical measures across 1015 ROIs between the group of patients with TLE and healthy subjects. Warm colors (red, orange, and yellow) indicate increases in TLE, while cool colors (blue) indicate decreases. Within-module connectivity is within-module z score of degree, and between-module connectivity is participation coefficient. Light gray areas represent gyri, and dark gray areas represent sulci. *Lat* = lateral, *Med* = medial.

an ROI, was increased both within and beyond the DMN, suggesting increased local interconnectedness. Within- and between-module connectivity is used to measure intermediate length and distant connections, respectively, and was decreased primarily in the DMN. We hypothesize that an increase in local structural connectivity may represent a compensatory, perhaps maladaptive, mechanism by which overall neural connectivity is maintained despite the loss of connections through important hub areas and explain the apparent contradiction between increased local connectivity and reduced long-range DMN connectivity. A mechanism suggested

by Vollmar et al (21) may reconcile this. They suggest that a loss of microstructural white matter integrity may lead to a dispersion of fiber directionality, reducing fractional anisotropy and long-range connectivity, which in turn leads to aberrant local network reorganization (21).

This structural connectivity investigation enhances the understanding of how functional connectivity is altered in TLE. Investigators in prior studies have used connectomics to study functional networks in TLE by using a variety of modalities, including electroencephalography (22), electrocorticography (23,24), and functional MR imaging

(3). Although the precise relationship between structural and functional connectivity is unclear, overall, our results are convergent with those of prior functional connectivity studies. For example, in prior functional MR imaging studies in TLE (3,4), decreased functional connectivity was observed between the medial orbitofrontal cortex and the posterior cingulate cortex, which we hypothesize relates to disrupted connectivity via the cingulum tract.

Bonilha et al (25) used a graph theoretical approach to study structural connectivity networks in TLE. Specifically, they used probabilistic tractography with diffusion-tensor imaging data

sets and solely focused on 20 cortical and subcortical brain regions primarily within the limbic system. They found reduced fiber density and increased local connectivity among these regions, which is concordant with findings in our study, but they did not include most of the cerebral cortex, including the DMN.

There are several limitations to the present study that merit further investigation. First, we recognize that the retrospective and cross-sectional design of this study limits our ability to determine cause-and-effect relationships between our observations and the clinical conditions we are describing. Second, we acknowledge that we cannot rule out a confounding effect of antiepileptic medications that may change diffusion properties. Given that some of the global measures of connectivity are unaffected in our population, we doubt this is a major factor, but we suggest conducting a prospective study that uses a generalized epilepsy population as a control group for more definitive study. Further, although there were no significant differences in participant characteristics, the age distributions of our two groups could be matched more closely. We also acknowledge that all patients in this study had left TLE, were referred from tertiary care centers, and were being evaluated for epilepsy surgery and therefore may not be representative of a more general TLE population. In addition, newer diffusion-weighted schemes (eg, Q-ball and diffusion spectrum imaging) may lead to more accurate tractography results, especially in areas with fiber crossings.

Acknowledgments: The authors acknowledge Nao Suzuki, BA, and Roberta Zanzonico, MD, for technical support, as well as Lawrence Wald, PhD, and Nikos Makris, PhD, for essential advice on diffusion acquisition and analysis.

Disclosures of Conflicts of Interest: M.N.D. No relevant conflicts of interest to disclose. L.D. No relevant conflicts of interest to disclose. N.T. No relevant conflicts of interest to disclose. C.R. Financial activities related to the present article: none to disclose. Financial activities not related to the present article: author received a consultancy from Sleep Med for the interpretation of clinical data and electroencephalograms. Other relationships: none to disclose. S.M.S. No relevant conflicts of interest to disclose.

References

- Mueller SG, Laxer KD, Cashdollar N, Buckley S, Paul C, Weiner MW. Voxel-based optimized morphometry (VBM) of gray and white matter in temporal lobe epilepsy (TLE) with and without mesial temporal sclerosis. *Epilepsia* 2006;47(5):900-907.
- Raichle ME, MacLeod AM, Snyder AZ, Powers WJ, Gusnard DA, Shulman GL. A default mode of brain function. *Proc Natl Acad Sci U S A* 2001;98(2):676-682.
- Liao W, Zhang Z, Pan Z, et al. Default mode network abnormalities in mesial temporal lobe epilepsy: a study combining fMRI and DTI. *Hum Brain Mapp* 2011;32(6):883-895.
- Pittau F, Grova C, Moeller F, Dubeau F, Gotman J. Patterns of altered functional connectivity in mesial temporal lobe epilepsy. *Epilepsia* 2012;53(6):1013-1023.
- Voets NL, Beckmann CF, Cole DM, Hong S, Bernasconi A, Bernasconi N. Structural substrates for resting network disruption in temporal lobe epilepsy. *Brain* 2012;135(Pt 8):2350-2357.
- Reinsberger C, Tanaka N, Cole AJ, et al. Current dipole orientation and distribution of epileptiform activity correlates with cortical thinning in left mesiotemporal epilepsy. *Neuroimage* 2010;52(4):1238-1242.
- Raj A, Mueller SG, Young K, Laxer KD, Weiner M. Network-level analysis of cortical thickness of the epileptic brain. *Neuroimage* 2010;52(4):1302-1313.
- Govindan RM, Makki MI, Sundaram SK, Juhász C, Chugani HT. Diffusion tensor analysis of temporal and extra-temporal lobe tracts in temporal lobe epilepsy. *Epilepsy Res* 2008;80(1):30-41.
- Ahmadi ME, Hagler DJ Jr, McDonald CR, et al. Side matters: diffusion tensor imaging tractography in left and right temporal lobe epilepsy. *AJNR Am J Neuroradiol* 2009;30(9):1740-1747.
- Bullmore E, Sporns O. Complex brain networks: graph theoretical analysis of structural and functional systems. *Nat Rev Neurosci* 2009;10(3):186-198.
- Hagmann P, Cammoun L, Gigandet X, et al. Mapping the structural core of human cerebral cortex. *PLoS Biol* 2008;6(7):e159.
- Chavez M, Valencia M, Navarro V, Latora V, Martinerie J. Functional modularity of background activities in normal and epileptic brain networks. *Phys Rev Lett* 2010;104(11):118701.
- Alexander-Bloch AF, Gogtay N, Meunier D, et al. Disrupted modularity and local connectivity of brain functional networks in childhood-onset schizophrenia. *Front Syst Neurosci* 2010;4:147.
- Dadducci A, Gerhard S, Griffa A, et al. The connectome mapper: an open-source processing pipeline to map connectomes with MRI. *PLoS One* 2012;7(12):e48121.
- Dale AM, Fischl B, Sereno MI. Cortical surface-based analysis. I. Segmentation and surface reconstruction. *Neuroimage* 1999;9(2):179-194.
- Fischl B, Sereno MI, Dale AM. Cortical surface-based analysis. II: Inflation, flattening, and a surface-based coordinate system. *Neuroimage* 1999;9(2):195-207.
- Desikan RS, Ségonne F, Fischl B, et al. An automated labeling system for subdividing the human cerebral cortex on MRI scans into gyral based regions of interest. *Neuroimage* 2006;31(3):968-980.
- Conturo TE, Lori NF, Cull TS, et al. Tracking neuronal fiber pathways in the living human brain. *Proc Natl Acad Sci U S A* 1999;96(18):10422-10427.
- Cheng H, Wang Y, Sheng J, et al. Characteristics and variability of structural networks derived from diffusion tensor imaging. *Neuroimage* 2012;61(4):1153-1164.
- Newman MEJ. Modularity and community structure in networks. *Proc Natl Acad Sci U S A* 2006;103(23):8577-8582.
- Vollmar C, O'Muircheartaigh J, Symms MR, et al. Altered microstructural connectivity in juvenile myoclonic epilepsy: the missing link. *Neurology* 2012;78(20):1555-1559.
- Baccalá LA, Alvarenga MY, Sameshima K, Jorge CL, Castro LH. Graph theoretical characterization and tracking of the effective neural connectivity during episodes of mesial temporal epileptic seizure. *J Integr Neurosci* 2004;3(4):379-395.
- van Dellen E, Douw L, Baayen JC, et al. Long-term effects of temporal lobe epilepsy on local neural networks: a graph theoretical analysis of corticography recordings. *PLOS ONE* 2009;4(11):e8081.
- Takahashi H, Takahashi S, Kanzaki R, Kawai K. State-dependent precursors of seizures in correlation-based functional networks of electrocorticograms of patients with temporal lobe epilepsy. *Neurol Sci* 2012;33(6):1355-1364.
- Bonilha L, Nesland T, Martz GU, et al. Medial temporal lobe epilepsy is associated with neuronal fibre loss and paradoxical increase in structural connectivity of limbic structures. *J Neurol Neurosurg Psychiatry* 2012;83(9):903-909.